Sandia National Laboratories

Guest Lecture Stanford ME469: SPD Computational Fluids Dynamics Research Interest

PRESENTED BY

Stefan P. Domino

Computational Thermal and Fluid Mechanics

Sandia National Laboratories

Sandia National Laboratories is a multimission laboratory managed and operated by National Technology & Engineering Solutions of Sandia, LLC, a wholly owned subsidiary of Honeywell International Inc., for the U.S. Department of Energy's National Nuclear Security Administration under contract DE-NA0003525.

2 SPD Computational Fluid Dynamics Research Interest: Outline

- Overview of Fluid Applications of Interest to SPD at Sandia National Labs
- Evolution of how Modeling/Simulation Shaped Fire Physics
- Multi-physics Coupling Examples
- Wind Applications and Other non-Reacting Examples
- Computational Scales of Interest
- Conclusions

3 Consider the Abnormal/Thermal Environment

- Characterized by a highly sooting, turbulent, reacting flow with Participating Media Radiation (PMR) and Conjugate Heat Transfer (CHT) mutiphysics coupling

Time-averaged (inset transient)

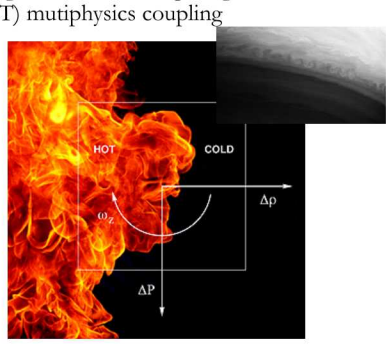

Vorticity generation

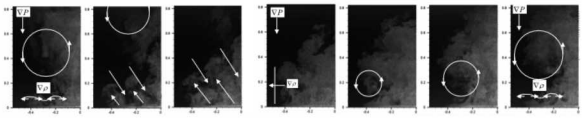

4 Evolution of a Mindset….. Cross Flow

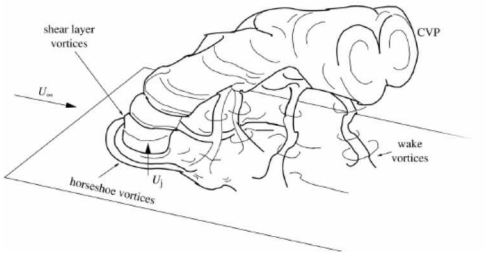

LES of pulsed jet in cross flow; Coussement et al, JFM, 2012

- Conclusion: The inclusion of a cross-flow wind profile couples vorticity of the pool and streamwise momentum which drives the formation of column vortices, increases the importance of mixing and, therefore, convective loads on the object become more important
- Change in mindset: Invest in Validation cases highlight the importance of convection physics

Ten meter (top) experiment and three meter (bottom) simulation

5 Evolution of a Mindset…..Whirling-like Flow

Brush fire (Curtin Springs, Australia)

Fire whirls from a 3-meter diameter pool in the Fire Laboratory for Accreditation of Modeling by Experiment, or FLAME, facility at Sandia National Laboratories. (Photo by Richard Simpson; A. Hanlin, lead experimentalist)

6 Several Buoyant Flow Examples

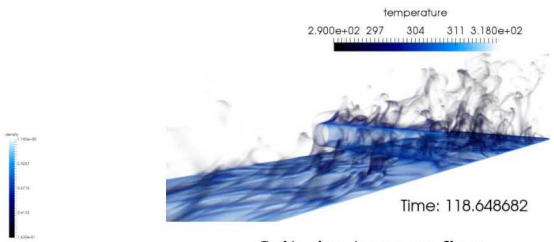

Cylinder in cross flow

Helium plume (low-/high-order)

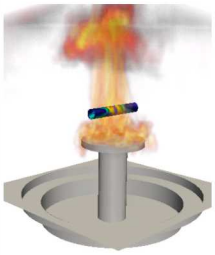

Object-in-fire

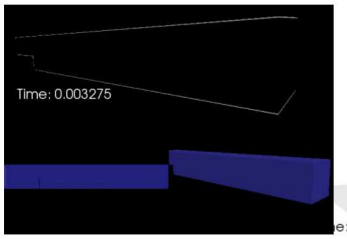

Heated backstep

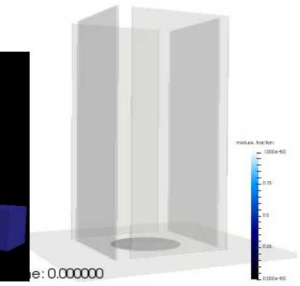

Whirling behavior

7 High Performance Computing (HPC) Enables Science

- Goal: Paint my house ASAP

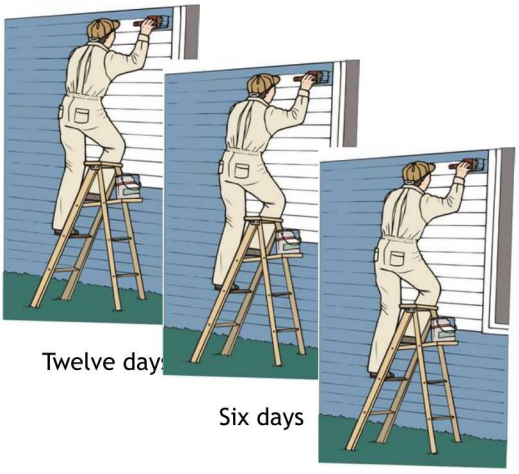

8 Wind Energy Applications… Towards Exascale

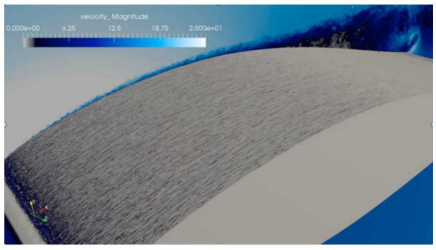

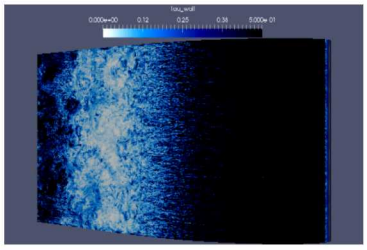

High Reynolds number flow past a wind energy turbine blade section
(Barone and Domino, 2016), ~1800 year simulation on one CPU

Late Roman Timeline
250 AD - 300 AD
250 AD: The Goths invade Anatolia (AKA, Asia Minor), in sea-borne raids they plunder *Nikopolis*

ECP EXASCALE COMPUTING PROJECT

9 Wind Energy Applications Including Blade-Resolved Simulations

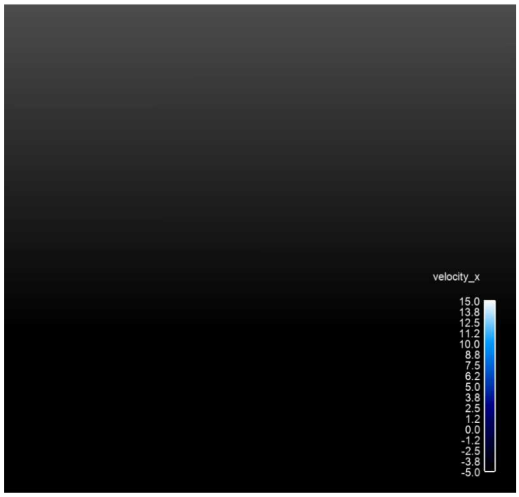

EXASCALE COMPUTING PROJECT

Vestas V27 225 kw wind turbine simulation

10 SPD Computational Fluid Dynamics Research Interest: Conclusion

- Interest ranges from turbulent, reacting flow (fires) to wind energy applications
- Multi-physics coupling allows for very complex fluid flow simulation and predictions
- Most engineering and "real-world" flows include a wide range of time and length scales
- HPC enables science and the pursuit of physics modeling and insight

Sandia National Laboratories

Guest Lecture Stanford ME469: Introduction to the low-Mach Number Approximation

PRESENTED BY

Stefan P. Domino

Computational Thermal and Fluid Mechanics

Sandia National Laboratories

U.S. DEPARTMENT OF ENERGY NNSA

Sandia National Laboratories is a multimission laboratory managed and operated by National Technology & Engineering Solutions of Sandia, LLC, a wholly owned subsidiary of Honeywell International Inc., for the U.S. Department of Energy's National Nuclear Security Administration under contract DE-NA0003525.

2 Introduction to the low-Mach Number Approximation: Outline

- Variable density, non-isothermal equation set
- DOF vs Equation count
- Non-dimensional form
- Asymptotic Expansion
- Derived low-Mach Equation Set
- The Role of Pressure
  - Motion and Thermodynamic
- Conclusions

3 Consider a Variable Density, non-Isothermal Fluid Flow System

- Consider the variable density (non-isothermal) equations of motion (momentum and continuity) with energy transport

$$\frac{\partial \rho}{\partial t} + \frac{\partial \rho u_j}{\partial x_j} = 0$$

$$\frac{\partial \rho u_i}{\partial t} + \frac{\partial \rho u_j u_i}{\partial x_j} - \frac{\partial \tau_{ij}}{\partial x_j} = \frac{\partial p}{\partial x_i}$$

$$\frac{\partial \rho E}{\partial t} + \frac{\partial \rho u_j H}{\partial x_j} - \frac{\partial u_i \tau_{ij}}{\partial x_j} = -\frac{\partial q_j}{\partial x_j}$$

2+nDim

+1

$$\rho = \frac{pM}{RT} \qquad \tau_{ij} = \mu\left(\frac{\partial u_i}{\partial x_j} + \frac{\partial u_j}{\partial x_i}\right) - \frac{2}{3}\mu\frac{\partial u}{\partial x_k}\delta_{ij} \qquad q_j = -\lambda\frac{\partial T}{\partial x_j}$$

$$E = \mathrm{H} - \frac{p}{\rho} \qquad H = \mathrm{h} + \frac{1}{2}u_i \qquad h = \int_{T^o}^{T} C_p dT$$

- See Paolucci (1982) or Baum (1978) for the low-Mach pedigree
- Number of Equations = (3+nDim) = Number of unknowns

- DOF
  - Density, ρ
  - Pressure, p
  - Velocity, u_i
  - Total energy, E
    - Total enthalpy, H
    - Static enthalpy, h
    - Temperature, T
- Properties:
  - Viscosity, μ
  - Specific heat, C_p
  - Thermal conductivity, λ
- Constitutive Relationships
  - Ideal gas law
  - Newtonian stress, τ_{ij}
  - Heat flux vector, q
  - Total enthalpy, H
  - Static enthalpy, h
  - CpdT

4 Dimensionless Form

- Non-dimensionalized by characteristic velocity and length scale

$$\frac{\partial \bar{\rho}}{\partial \bar{t}} + \frac{\partial \bar{\rho}\bar{u}_j}{\partial \bar{x}_j} = 0$$

$$\frac{\partial \bar{\rho}\bar{u}_i}{\partial \bar{t}} + \frac{\partial \bar{\rho}\bar{u}_j\bar{u}_i}{\partial \bar{x}_j} + \frac{1}{\gamma M_a^2}\frac{\partial \bar{p}}{\partial \bar{x}_i} = \frac{1}{R_e}\frac{\partial \bar{\tau}_{ij}}{\partial \bar{x}_j}$$

$$\frac{\partial \bar{\rho}\bar{h}}{\partial \bar{t}} + \frac{\partial \bar{\rho}\bar{u}_j\bar{h}}{\partial \bar{x}_j} = -\frac{1}{P_r R_e}\frac{\partial \bar{q}_j}{\partial \bar{x}_j} + \frac{\gamma-1}{\gamma}\frac{\partial \bar{p}}{\partial \bar{t}} + \frac{\gamma-1}{\gamma}\frac{M_a^2}{R_e}\frac{\partial \bar{u}_i\bar{\tau}_{ij}}{\partial \bar{x}_j} - \frac{\gamma-1}{\gamma}M_a^2\left(\frac{\partial \bar{\rho}\bar{u}_k\bar{u}_k}{\partial \bar{x}_j} + \frac{\partial \bar{\rho}\bar{u}_j\bar{u}_k\bar{u}_k}{\partial \bar{x}_j}\right)$$

$$R_e = \frac{\rho_\infty U_\infty L}{\mu_\infty} \qquad P_r = \frac{C_{p\infty}\mu_\infty}{\lambda_\infty} \qquad M_a = \sqrt{\frac{U_\infty^2}{\gamma RT_\infty/M}}$$

- Note:
  - As Mach number approaches zero, viscous work and kinetic energy terms become negligible
  - However, momentum equation seems to become singular (pressure gradient term)
- To explore the singularity, write each DOF as an asymptotic series:

$$\bar{p} = \bar{p}_o + \bar{p}_1\epsilon + \bar{p}_2\epsilon^2 + \dots \qquad \frac{\partial \bar{p}_o}{\partial \bar{t}} + \frac{\partial \bar{p}_o\bar{u}_j^o}{\partial \bar{x}_j} = 0$$

$$\bar{u}_i = \bar{u}_i^o + \bar{u}_i^1\epsilon + \bar{u}_i^1\epsilon^2 + \dots$$

$$\bar{T} = \bar{T}_o + \bar{T}_1\epsilon + \bar{T}_2\epsilon^2 + \dots \qquad \frac{\partial \overline{\bar{u}_i^o\rho_o}}{\partial \bar{t}} + \frac{\partial \bar{p}_o\overline{\bar{u}_i^o u_j^o}}{\partial \bar{x}_j} + \frac{1}{\gamma M_a^2}\frac{\partial \bar{p}_o}{\partial \bar{x}_i} = 0$$

5 Exploration of the Pressure Singularity

- To explore the singularity, write each DOF as an asymptotic series:

$$\bar{p} = \bar{p}_o + \bar{p}_1\epsilon + \bar{p}_2\epsilon^2 + \dots$$

$$\bar{u}_i = \bar{u}_{o,i} + \bar{u}_{1,i}\epsilon + \bar{u}_{1,i}\epsilon^2 + \dots$$

$$\bar{T} = \bar{T}_o + \bar{T}_1\epsilon + \bar{T}_2\epsilon^2 + \dots$$

- The resulting zeroeth-order equations are as follows:

$$\frac{\partial \bar{\rho}_o}{\partial \bar{t}} + \frac{\partial \bar{\rho}_o \bar{u}_{o,j}}{\partial \bar{x}_j} = 0$$

$$\frac{\partial \bar{\rho}_o \bar{u}_{o,i}}{\partial \bar{t}} + \frac{\partial \bar{\rho}_o \bar{u}_{o,j}\bar{u}_{o,i}}{\partial \bar{x}_j} + \frac{1}{\gamma M_a^2}\left(\frac{\partial \bar{p}_o}{\partial \bar{x}_i} + \epsilon\frac{\partial \bar{p}_1}{\partial \bar{x}_i}\right) = \frac{1}{R_e}\frac{\partial \bar{\tau}_{o,ij}}{\partial \bar{x}_j}$$

$$\frac{\partial \bar{\rho}_o \bar{h}_o}{\partial \bar{t}} + \frac{\partial \bar{\rho} \bar{u}_{o,j}\bar{h}_o}{\partial \bar{x}_j} = -\frac{1}{P_r R_e}\frac{\partial \bar{q}_{o,j}}{\partial \bar{x}_j} + \frac{\gamma-1}{\gamma}\frac{\partial \bar{p}_o}{\partial \bar{t}}$$

- In order for the zeroeth-order momentum equation to be well conditioned in the limit of zero Mach number, $\frac{\partial \bar{p}_o}{\partial \bar{x}_i}$ must be spatially zero with $\epsilon = \gamma M_a^2$
- p_o is the constant-in-space, possibly variable in time thermodynamic pressure
- p_1 is the variable is space pressure, which is also known as the "motion pressure"

6 The Final low-Mach Number Equation Set

- In dimensional form, the low-Mach system is as follows:

$$\frac{\partial \rho}{\partial t} + \frac{\partial \rho u_j}{\partial x_j} = 0$$

$$\frac{\partial \rho u_i}{\partial t} + \frac{\partial \rho u_j u_i}{\partial x_j} - \frac{\partial \tau_{ij}}{\partial x_j} = \frac{\partial p^d}{\partial x_i}$$

$$\frac{\partial \rho h}{\partial t} + \frac{\partial \rho u_j h}{\partial x_j} = -\frac{\partial q_j}{\partial x_j} + \frac{\partial p^t}{\partial t}$$

2+nDim

$$\rho = \frac{p^t M}{RT} \qquad \tau_{ij} = \mu\left(\frac{\partial u_i}{\partial x_j} + \frac{\partial u_j}{\partial x_i}\right) - \frac{2}{3}\mu\frac{\partial u}{\partial x_k}\delta_{ij}$$

$$q_j = -\lambda\frac{\partial T}{\partial x_j} \qquad h = \int_{T^o}^{T} C_p dT$$

- Ramifications?
  - We have effectively filtered out the acoustics, i.e., the wave speed is infinitely fast
  - Continuity is met over any finite length instantly
  - DOF/Equation system is: ρ, p^d, u_i, h; p^t is a constant for an open domain
  - In practice, a functional form for the dynamic pressure is derived:

$$\frac{\partial \rho}{\partial t} + \frac{\partial \rho u_j}{\partial x_i} - \frac{\partial}{\partial x_i}\tau\frac{\partial}{\partial x_i}\Delta p^d = 0 \quad \text{- or } \quad \frac{\partial}{\partial x_i}\left(\frac{\partial \rho u_i}{\partial t} + \cdots\right)$$

Pressure Poisson Equation (PPE)

- DOF
  - Density, ρ
  - Pressure, p^d
  - Velocity, u_i
  - Total energy, E
    - Total enthalpy, H
    - Static enthalpy, h
    - Temperature, T
- Properties:
  - Viscosity, μ
  - Specific heat, C_p
  - Thermal conductivity, λ
- Constitutive Relationships
  - Ideal gas law
  - Newtonian stress, τ_{ij}
  - Heat flux vector, q
  - Total enthalpy, H
  - Static enthalpy, h
  - CpdT

7 Introduction to the low-Mach Number Approximation: Conclusions

- Variable density, non-isothermal equation set allow for all length and time scales for a given physics
- For a low-Mach flow, the density and pressure are not coupled by an equation of state
- The low-Mach procedure filters the acoustics, which can not be of prime interest in the flow

Sandia National Laboratories

Guest Lecture Stanford ME469: Common low-Mach Discretization Approaches

PRESENTED BY

Stefan P. Domino

Computational Thermal and Fluid Mechanics

Sandia National Laboratories

U.S. DEPARTMENT OF ENERGY NNSA

Sandia National Laboratories is a multimission laboratory managed and operated by National Technology & Engineering Solutions of Sandia, LLC, a wholly owned subsidiary of Honeywell International Inc., for the U.S. Department of Energy's National Nuclear Security Administration under contract DE-NA0003525.

2 Common low-Mach Discretization Approaches: Outline

- Cell-centered Finite Volume (FV)
- Edge-based Vertex-Centered (EBVC)
- Finite Element Method (FEM)
- Control-Volume Finite Element Method (CVFEM)
- Staggered arrangement
- Conclusions

3 Equal-Order Interpolation Cell-Centered (CC) Finite Volume

- All primitives are collocated at the cell-center of the element with equal-order interpolation
- Classic two-state, "L" and "R" approach provides spatially second-order accuracy

▲ Surface quadrature point

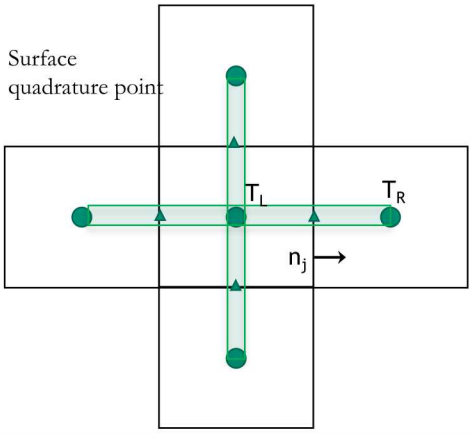

- Consider a simple heat conduction model PDE

$$\rho C_p \frac{\partial T}{\partial t} - \frac{\partial}{\partial x_j}\lambda\frac{\partial T}{\partial x_j} = 0$$

- Integrate over a control volume and use Gauss-Divergence

$$\int \rho C_p \frac{\partial T}{\partial t} dV - \int \lambda \frac{\partial T}{\partial x_j} n_j \, dS = 0$$

with: $$\frac{\partial T}{\partial x_j} = \frac{(T_R - T_L)n_j}{\|\Delta x_j\|}$$

- Iterate element cell-centers for volume contributions
- Iterate element faces for surface flux contribution

4 Equal Order Interpolation Edge-Based Vertex-Centered (EBVC) Finite Volume

- All primitives are collocated at the vertices of the elements with equal-order interpolation
- A dual mesh is constructed to obtain flux and volume quadrature locations
- Classic two-state, "L" and "R" approach provides spatially second-order accuracy

▲ Surface quadrature point (area summed to edge)

◆ Volume quadrature point (sub-vol summed to node)

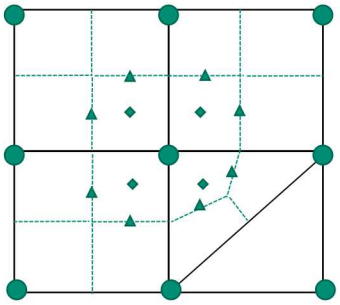

Dual-volume definition

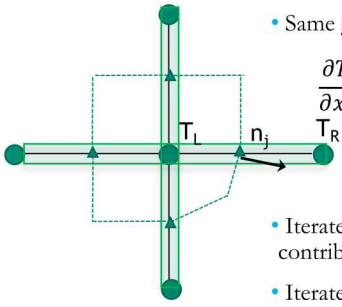

Edge-based stencil

- Same grad-op as CC

$$\frac{\partial T}{\partial x_j} = \frac{(T_R - T_L)n_j}{\|\Delta x_j\|}$$

- Iterate nodes for volume contributions
- Iterate edges for surface flux contribution

5 Typical Failings for Two-State Discretization Methods

- With two points, only a linear basis can be used.
- Therefore, CC and EBVC are limited to second-order spatial accuracy
- Non-orthogonality is problematic for gradient-operator

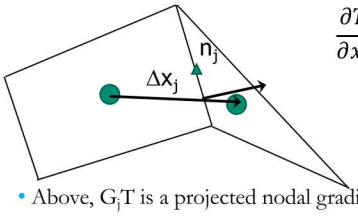

$$\frac{\partial T}{\partial x_j} = G_j T + \left[(T_R - T_L) - G_k T \Delta x_k\right] \frac{A_j}{A_l \Delta x_l}$$

With area vector defined by: $A_j = n_j dS$

- Above, $G_j T$ is a projected nodal gradient at the cell-center, or vertex center:
- Non-orthogonality is simply defined as the mis-alignment of the distance vector between the two "L" and "R" states and the surface normal
- Both edge- and cell centered-based schemes show degraded accuracy on typical production meshes.
- Several non-orthogonality approaches are available, see Jasek's Imperial College Dissertation for a complete description

$$G_j T = \frac{\int T A_j}{\int dV}$$

6 The Finite Element Method (FEM)

- Consider an alternative approach in which a finite element method (FEM) is employed
- Define an underlying nodal basis with the element:

$$T(x_j) = \sum_{i=1}^{npe} N_i(x_j) T_i \qquad \frac{\partial T}{\partial x_j} = \sum_{i=1}^{npe} \frac{\partial N_i(x_j)}{\partial x_j} T_i$$

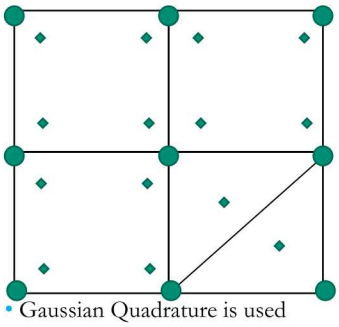

- Gaussian Quadrature is used
- On a -1:1 range, +/- sqrt(3)/3

- Consider a simple heat conduction model PDE

$$\rho C_p \frac{\partial T}{\partial t} - \frac{\partial}{\partial x_j} \lambda \frac{\partial T}{\partial x_j} = 0$$

- Integrate using a test function,

$$\int w \rho C_p \frac{\partial T}{\partial t} dV - \int w \frac{\partial}{\partial x_j} \lambda \frac{\partial T}{\partial x_j} dV = 0$$

- Integration-by-parts provides:

$$\int w \rho C_p \frac{\partial T}{\partial t} dV + \int \frac{\partial w}{\partial x_j} \lambda \frac{\partial T}{\partial x_j} dV + \int w \lambda \frac{\partial T}{\partial x_j} n_j dS = 0$$

- Iterate element quadrature points
- Note that N can be arbitrary in order (shown here for a linear)

7 The Hybird Control-Volume Finite Element Method (CVFEM)

- A combination between the edge-based vertex-centered and FEM is the method known as Control Volume Finite Element ()
- A dual mesh is constructed to obtain flux and volume quadrature locations
- As with FEM, a basis is defined:

$$T(x_j) = \sum_{i=1}^{npe} N_i(x_j) T_i \qquad \frac{\partial T}{\partial x_j} = \sum_{i=1}^{npe} \frac{\partial N_i(x_j)}{\partial x_j} T_i$$

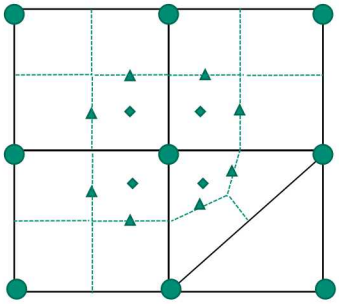

Dual-volume definition

- Integration-by-parts over test function w:

$$\int w\rho C_p \frac{\partial T}{\partial t} dV + \int \frac{\partial w}{\partial x_j} \lambda \frac{\partial T}{\partial x_j} dV + \int w\, \lambda \frac{\partial T}{\partial x_j} n_j dS = 0$$

- However, define a test function, w, as a piece-wise constant function (Heavyside) to be 1 inside the dual volume and 0 outside. Gradient is a dirac-delta function:

$$\frac{\partial w}{\partial x_j} = -n_j \delta(x_j - ip_j)$$

- Leading to:

$$\int \rho C_p \frac{\partial T}{\partial t} dV - \int \lambda \frac{\partial T}{\partial x_j} n_j \, dS = 0$$

8 Control-Volume Finite Element Method Attributes

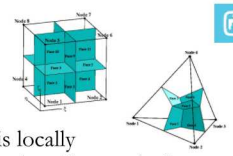

- The CVFEM method, therefore, is a finite volume scheme that is locally conservative, i.e., momentum leaving one dual volume face enters the adjacent dual volume
- However, the gradient operator, like its FEM counterpart is absent of any error due to non-orthogonality
- Since the test-function, w, is different from the underlying basis representation, this method can be considered a Petrov-Galerkin method
- The method can also be promoted in polynomial space

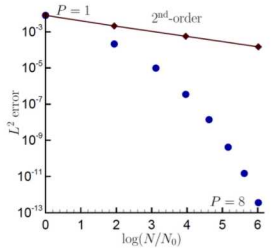

Spectral convergence

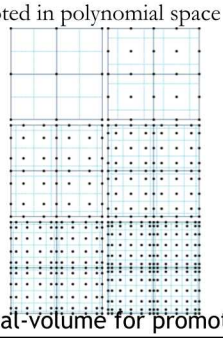

Dual-volume for promoted quad4

P=1 (left) and P=4 (right)
Helium plume (VR-density)

9 Classic Staggered Finite Volume

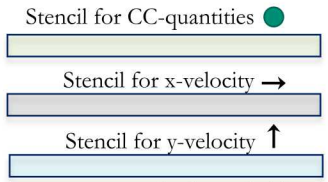

- Velocity degree-of-freedom is staggered relative to pressure and other primitives, e.g., enthalpy, mixture fraction, etc.

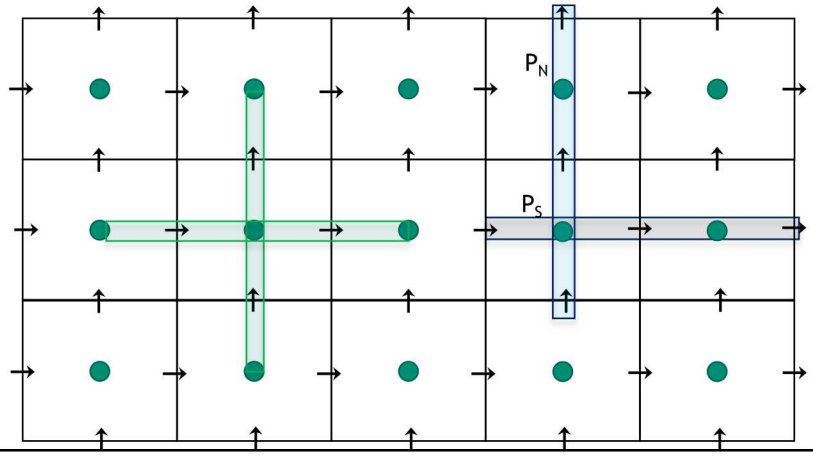

10 Attributes of a Staggered Scheme

- By design, non-orthogonality is absent, however, complex geometry will be stair-stepped
- From a fluids perspective, the operators are ideal, i.e., pressure gradient for momentum is compact, e.g., $(P_E - P_W)\Delta x^{-1}$
  - As will be seen in future lecture topics, the skew-adjoint nature of the Divergence operator, **D**, and Gradient operator, **G**, allows for a Laplace operator, **L** = **DG**
- Can be extended to higher-order
- Frequently, meshing complex geometries can be extremely difficult (consider our V27 example)

11 Common low-Mach Discretization Approaches: Conclusions

- Two-state methods, e.g., cell-centered and EBVC are attractive due to simplicity, however, suffer from non-orthogonality issues in the diffusion operator
- FEM provides a machinery to provide accurate discretizations on non-ideal meshes, however, the same diffusion operator suffers on high-aspect ratio meshes
- CVFEM is a hybrid method that contains the likeable attributes of both FV and FEM
- Staggered arrangement is well suited for a class of fluid mechanics applications where low-order or simple geometries are found

Sandia National Laboratories

Guest Lecture Stanford ME469: Splitting and Stabilization Errors

PRESENTED BY

Stefan P. Domino

Computational Thermal and Fluid Mechanics

Sandia National Laboratories

U.S. DEPARTMENT OF ENERGY NNSA

Sandia National Laboratories is a multimission laboratory managed and operated by National Technology & Engineering Solutions of Sandia, LLC, a wholly owned subsidiary of Honeywell International Inc., for the U.S. Department of Energy's National Nuclear Security Administration under contract DE-NA0003525.

2 Splitting and Stabilization Errors: Outline

- Block Matrix and Operator Form
- Approximate Factorization
- Splitting Errors
- Stabilization Errors
- Detailed Code Verification
- Conclusions

3 Introduction to Block Matrix Form

- Consider the monolithic, uniform density, low-Mach equation system:

$$\frac{\partial u_j}{\partial x_j} = 0$$

$$\frac{\partial \rho u_i}{\partial t} + \frac{\partial \rho u_j u_i}{\partial x_j} - \frac{\partial \rho \tau_{ij}}{\partial x_j} = \frac{\partial p_i}{\partial x_i} + S_i$$

that can be written in block form as:

$$\begin{bmatrix} A & G \\ D & 0 \end{bmatrix} \begin{bmatrix} u^{n+1} \\ p^{n+1} \end{bmatrix} = \begin{bmatrix} f \\ 0 \end{bmatrix}$$

- We seek to factorize this system via:

$$\begin{bmatrix} A & G \\ D & 0 \end{bmatrix} \approx \begin{bmatrix} A & 0 \\ D & B_1 \end{bmatrix} \begin{bmatrix} I & B_2 \\ 0 & I \end{bmatrix} \approx \begin{bmatrix} A & AB_2G \\ D & (B_1 + DB_2G) \end{bmatrix} \begin{bmatrix} u^{n+1} \\ p^{n+1} \end{bmatrix} = \begin{bmatrix} f \\ 0 \end{bmatrix}$$

the exact factorization can be recovered by defining: $B_2 = A^{-1}$, $B_1 = -DB_2G$

- $\mathbf{B_2}$ determines the projection time scale, choose to approximate $\mathbf{A^{-1}}$
- $\mathbf{B_1}$ controls the projection error, choose to cancel $\mathbf{BD_2G}$

4 Introduction to Block Matrix Form

- The approximate factorization

$$\begin{bmatrix} A & G \\ D & 0 \end{bmatrix} \approx \begin{bmatrix} A & 0 \\ D & B_1 \end{bmatrix} \begin{bmatrix} I & B_2 \\ 0 & I \end{bmatrix} \approx \begin{bmatrix} A & AB_2G \\ D & (B_1 + DB_2G) \end{bmatrix} \begin{bmatrix} u^{n+1} \\ p^{n+1} \end{bmatrix} = \begin{bmatrix} f \\ 0 \end{bmatrix}$$

- can be written now as two segregated steps:

Momentum and Continuity: $\begin{bmatrix} A & 0 \\ D & B_1 \end{bmatrix} \begin{bmatrix} \hat{u} \\ \hat{p} \end{bmatrix} = \begin{bmatrix} f \\ 0 \end{bmatrix}$ $\Rightarrow$ $A\hat{u} = f$, $D\hat{u} + B_1\hat{p} = 0$

Nodal Projection: $\begin{bmatrix} I & B_2 \\ 0 & I \end{bmatrix} \begin{bmatrix} u^{n+1} \\ p^{n+1} \end{bmatrix} = \begin{bmatrix} \hat{u} \\ \hat{p} \end{bmatrix}$ $\Rightarrow$ $u^{n+1} = \hat{u} - B_2 p^{n+1} = 0$, $p^{n+1} = \hat{p}$

- This approach seems to be straight forward, however, what errors have we introduced by this procedure of splitting the monolithic (fully coupled) system?

$$\begin{bmatrix} A & G \\ D & 0 \end{bmatrix} \begin{bmatrix} u^{n+1} \\ p^{n+1} \end{bmatrix} = \begin{bmatrix} f \\ 0 \end{bmatrix} + \begin{bmatrix} (I - AB_2)Gp^{n+1} \\ -(B_1 + DB_2G)p^{n+1} \end{bmatrix}$$ Exact iff: $B_2 = A^{-1}$, $B_1 = -DB_2G$

- In most cases, $\mathbf{B_2}$ is approximately $\mathbf{A^{-1}}$ and a first-order temporal splitting error is noted

5 Incremental Pressure-Projection without Pressure Stabilization

- Let the inverse of **A**, $\mathbf{A}^{-1}$ be approximated by $\mathbf{B}_2$ as a scalar, $\boldsymbol{\tau}$
- Let $\mathbf{B}_1$ be equal to the Laplace operator, **-L**

Momentum and Continuity:

$$\begin{bmatrix} A & 0 \\ D & -\tau L \end{bmatrix}\begin{bmatrix} \hat{u} \\ p^{n+1} \end{bmatrix} = \begin{bmatrix} f \\ -\tau L p^n \end{bmatrix} \quad \begin{cases} A\hat{u} = f - Gp^n \\ D\hat{u} - \tau L(p^{n+1} - p^n) = 0 \end{cases}$$

Nodal Projection:

$$\begin{bmatrix} I & \tau G \\ 0 & I \end{bmatrix}\begin{bmatrix} u^{n+1} \\ p^{n+1} \end{bmatrix} = \begin{bmatrix} \hat{u} \\ \hat{p} \end{bmatrix} + \begin{bmatrix} \tau G p^n \\ 0 \end{bmatrix} \quad \begin{cases} u^{n+1} = \hat{u} - \tau G(p^{n+1} - p^n) \\ p^{n+1} = \hat{p} \end{cases}$$

- The new splitting and stabilization error is given by:

$$\begin{bmatrix} A & G \\ D & 0 \end{bmatrix}\begin{bmatrix} u^{n+1} \\ p^{n+1} \end{bmatrix} = \begin{bmatrix} f \\ 0 \end{bmatrix} + \begin{bmatrix} (I - A\tau)G(p^{n+1} - p^n) \\ \tau(L - DG)(p^{n+1} - p^n) \end{bmatrix}$$

Examples:
- Dwyer (1990)
- Almgren (2000)

- The above can be shown to deomstrate second-order temporal error (coming)
- A scheme can be designed such that **L** = **DG** (staggered)
- A scheme in which **L** != **DG** (collocated or equal-order) can show that **L-DG** ~ 4th-order pressure stabilization

6 The Role of Pressure Stabilization (L!=DG) in an Equal-Order Approach

- Consider the classic lid-driven cavity flow with top wall velocity of Uo

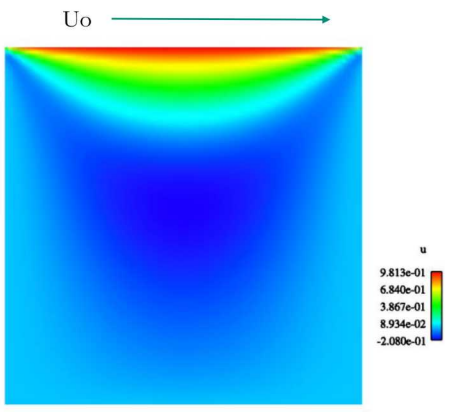

lid-driven cavity velocity (u-component)

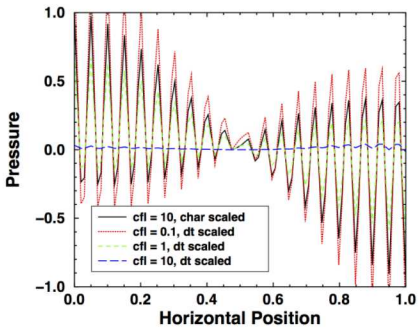

Unsmoothed pressure field at various Courant numbers

7

Incremental Approximate Pressure-Projection with Pressure Stabilization Errors

- Let the inverse of **A**, $\mathbf{A}^{-1}$ be approximated by $\mathbf{B}_2$ as a scalar, $\boldsymbol{\tau}$
- Let $\mathbf{B}_1$ be equal to the Laplace operator, -**L**

Momentum and Continuity: $\begin{bmatrix} A & 0 \\ D & -\tau L \end{bmatrix}\begin{bmatrix} \hat{u} \\ p^{n+1} \end{bmatrix} = \begin{bmatrix} f \\ -D\tau G p^n \end{bmatrix}$ $\begin{matrix} A\hat{u} = f - Gp^n \\ D\hat{u} = \tau(Lp^{n+1} - DGp^n) \end{matrix}$

Nodal Projection: $\begin{bmatrix} I & \tau G \\ 0 & I \end{bmatrix}\begin{bmatrix} u^{n+1} \\ p^{n+1} \end{bmatrix} = \begin{bmatrix} \hat{u} \\ \hat{p} \end{bmatrix} + \begin{bmatrix} \tau G p^n \\ 0 \end{bmatrix}$ $\begin{matrix} u^{n+1} = \hat{u} - \tau G(p^{n+1} - p^n) \\ p^{n+1} = \hat{p} \end{matrix}$

- The new splitting and stabilization error is given by:

$$\begin{bmatrix} A & G \\ D & 0 \end{bmatrix}\begin{bmatrix} u^{n+1} \\ p^{n+1} \end{bmatrix} = \begin{bmatrix} f \\ 0 \end{bmatrix} + \begin{bmatrix} (I - A\tau)G(p^{n+1} - p^n) \\ \tau(L - DG)p^{n+1} \end{bmatrix}$$

Examples:
- Rhie-Chow (1983)
- Peric (1985)

- The above can be shown to hold a second-order temporal error (coming)
- Here, due to equal-order interpolation, i.e., collocation of primitives, **L** != **DG**
- Therefore, **L-DG** ~ 4th-order pressure stabilization (pressure oscillations damped)
- Therefore, pressure-stabilization remains

8

Monolithic Staggered or Equal-order Interpolation (Collocated)

- Note that we need not split the system for a staggered scheme:

$$\begin{bmatrix} A & G \\ D & -\tau L \end{bmatrix}\begin{bmatrix} u^{n+1} \\ p^{n+1} \end{bmatrix} = \begin{bmatrix} f \\ -\tau L p^n \end{bmatrix}$$

$$\begin{bmatrix} A & G \\ D & 0 \end{bmatrix}\begin{bmatrix} u^{n+1} \\ p^{n+1} \end{bmatrix} = \begin{bmatrix} f \\ 0 \end{bmatrix} + \begin{bmatrix} 0 \\ \tau(L - DG)(p^{n+1} - p^n) \end{bmatrix}$$

- or collocated:

$$\begin{bmatrix} A & G \\ D & 0 \end{bmatrix} \approx \begin{bmatrix} A & G \\ D & -\tau L \end{bmatrix}\begin{bmatrix} u^{n+1} \\ p^{n+1} \end{bmatrix} = \begin{bmatrix} f \\ -\tau DG p^n \end{bmatrix}$$

$$\begin{bmatrix} A & G \\ D & 0 \end{bmatrix}\begin{bmatrix} u^{n+1} \\ p^{n+1} \end{bmatrix} = \begin{bmatrix} f \\ 0 \end{bmatrix} + \begin{bmatrix} 0 \\ \tau(L - DG)p^{n+1} \end{bmatrix}$$

- Conclusion: Monolithic schemes control splitting error, however, dealing with pressure stabilization is an additional complexity for equal-order methods

9 The Choice of the B_1 can Vary by The Method..

- In Pressure-Stabilized Petrov-Galerkin methods (Hughes et al, 1985):

$$\begin{bmatrix} A & G \\ D & -\tau \nabla w \cdot M \end{bmatrix} \begin{bmatrix} u^{n+1} \\ p^{n+1} \end{bmatrix} = \begin{bmatrix} f \\ 0 \end{bmatrix}$$

- Here, **M** is a fine scale momentum residual and w is the test function for the Finite Element Method
- Note that **M** contains a local pressure gradient which, thereby, provides the pressure stabilization
- The fine-scale momentum residual is evaluated locally at the quadrature point and with mesh refinement reduces at a design-order rate
- With some algebra, one can show that **L-DG ~ M**
- For more references, see Magumdar, Numerical Heat Transfer, 1988

10 Code Verification To Establish Accuracy

- Consider a two-dimensional transient solution to the incompressible equations of motion:
- This solution is known as the convecting, decaying, Taylor vortex

$$u = u^o - \cos\big(\pi(x - u^o t)\big) \sin\big(\pi(y - v^o t)\big)\, e^{-2\omega t}$$

$$v = v^o + \sin\big(\pi(x - u^o t)\big) \cos\big(\pi(y - v^o t)\big)\, e^{-2\omega t}$$

$$\mathrm{p} = -\frac{p^o}{4}\big[\,(\cos\big(2\pi(x - u^o t)\big) + \cos(\,\pi(y - v^o t))\big] e^{-4\omega t}$$

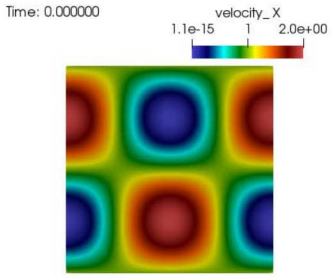

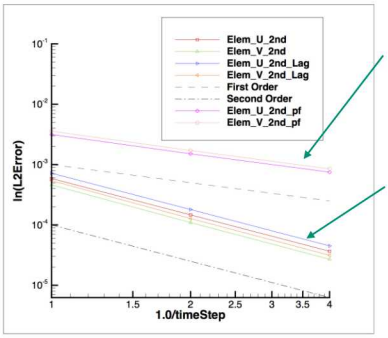

Approximate factorization

Flavors of incremental

11 Splitting and Stabilization Errors: Conclusion

- Block matrix and operator form represents a useful construct to analyze coupling and stabilization
- Approximate Factorization is generally $O(\Delta t)$
- With very simple modifications, splitting error is mitigated
- Detailed code verification is a critical tool to both test theoretical understandings in addition to establishing a proper code implementation

Sandia National Laboratories

Guest Lecture Stanford ME469: Advection Operators

PRESENTED BY

Stefan P. Domino

Computational Thermal and Fluid Mechanics

Sandia National Laboratories

U.S. DEPARTMENT OF ENERGY NNSA

Sandia National Laboratories is a multimission laboratory managed and operated by National Technology & Engineering Solutions of Sandia, LLC, a wholly owned subsidiary of Honeywell International Inc., for the U.S. Department of Energy's National Nuclear Security Administration under contract DE-NA0003525.

2 Advection Operators: Outline

- Classic Analysis on Advection/Diffusion/Time Scalar Transport
- The Role of Diagonal Dominance
- Upwind Methods
- Linear Residual-Based Stabilization
- Nonlinear Residual-Based Stabilization
- Conclusions

3 Consider a Simple Advection/Diffusion/Time Scalar Transport

- PDE is given by: $\frac{\partial \rho Z}{\partial t} + \frac{\partial \rho u_j Z}{\partial x_j} - \frac{\partial}{\partial x_j}\frac{\mu}{Sc}\frac{\partial Z}{\partial x_j} = 0$
- Integral form: $\int \frac{\partial \rho Z}{\partial t} dV + \int \left[\rho u_j Z - \frac{\mu}{Sc}\frac{\partial Z}{\partial x_j}\right] n_j \, dS = 0$
- Discrete form: $\sum_{sip} \frac{(\rho Z^{n+1} - \rho Z^n)}{\Delta t} dV + \sum_{ip} \dot{m} Z_{ip} - \sum_{ip} \frac{\mu}{Sc}\frac{\partial Z}{\partial x_j} n_j \mathrm{dS}$
- Matrix Form: $(-a_{j-1} \quad a_j \quad -a_{j+1}) \begin{pmatrix} Z_{j-1} \\ Z_j \\ Z_{j+1} \end{pmatrix} = 0$

$$a_{j+1} = \frac{\mu}{Sc}\frac{A}{\Delta x} - \frac{\dot{m}_{j+1/2}}{2} \qquad a_{j-1} = \frac{\mu}{Sc}\frac{A}{\Delta x} + \frac{\dot{m}_{j-1/2}}{2}$$

$$a_j = a_{j+1} + a_{j-1} + (\dot{m}_{j+1/2} - \dot{m}_{j-1/2}) + \frac{\rho \Delta V}{\Delta t}$$

$$\frac{\sum_{i \neq j} |a_{ij}|}{|a_{ii}|} \leq 1$$

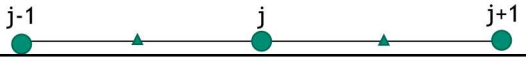

4 Diagonal Dominance Check

- For a monotonic operator: $DD = \frac{\sum_{i \neq j} |a_{ij}|}{|a_{ii}|} \leq 1$
- Consider u = 1 cm/s; ρ = 1.2e-3 g/cm3; μ/Sc = 1.8e-5 g/cm-s; Δx = 0.1 cm; ; Δt >> 1:
  - a_{j+1}=1.2e-3 a_{j-1}=2.4e-3 a_j = 3.6e-3 $\quad DD \leq 1$
  - Stable and monotonic field will be realized
- Consider u = 10 cm/s; ρ = 1.2e-3 g/cm3; μ/Sc = 1.8e-5 g/cm-s; Δx = 0.1 cm; Δt >> 1:
  - a_{j+1}=-4.2e-3 a_{j-1}=7.8e-3 a_j = 3.6e-3 $\quad DD > 1$
  - Unstable and lack of scalar monotonicity will be realized
  - Standard preconditioner, e.g., SGS, are not expected to converge the linear system
- Mesh spacing for monotonicity must be: $\Delta x \leq \frac{2\mu/Sc}{\rho u} \quad Pe = \frac{\rho u \Delta x}{\mu/Sc} \leq 2$
  - Cell Peclet number, Pe is a cell-Reynolds number based on local properties and mesh spacing
- Consider u = 10 cm/s; ρ = 1.2e-3 g/cm3; μ/Sc = 1.8e-5 g/cm-s; Δx = 0.1 cm; Δt =?
  - For diagonal dominance, Δt = 0.0143 which corresponds to a Courant number of 0.012! $C = \frac{u\Delta t}{\Delta x}$

5 Upwinding Operators

- Upwind advection operators can provide diagonal dominance (at the cost of accuracy)

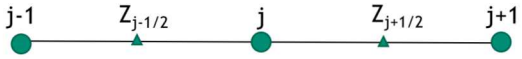

$$Z_{j+1/2} = \begin{cases} Z_j; u > 0 \\ Z_{j+1}; u < 0 \end{cases}$$

- However, upwind operators, even if higher-order, are numerically diffuse

- Higher-order upwind can be obtained on an unstructured mesh by use of projected nodal gradients and extrapolation:

$$G_x Z_j = \frac{Z_{j+1} - Z_{j-1}}{2\Delta x} \qquad G_x Z_{j-1} = \frac{Z_j - Z_{j-2}}{2\Delta x}$$

for u>0

$$Z_{j+1/2} = \propto \left(Z_j + G_x Z_j \frac{\Delta x}{2}\right) + (1 - \propto)\left[\frac{1}{2}(Z_j + Z_{j+1})\right]$$

$$Z_{j-1/2} = \propto \left(Z_{j-1} + G_x Z_{j-1} \frac{\Delta x}{2}\right) + (1 - \propto)\left[\frac{1}{2}(Z_j + Z_{j-1})\right]$$

α is a blending parameter

6 Higher-order Upwinding

- Blending extrapolated upwind with central $(Z_L+Z_R)/2$ provides:

for u>0

$$Z_{j+1/2} = \propto \left(Z_j + G_x Z_j \frac{\Delta x}{2}\right) + (1 - \propto)\left[\frac{1}{2}(Z_j + Z_{j+1})\right]$$

$$Z_{j-1/2} = \propto \left(Z_{j-1} + G_x Z_{j-1} \frac{\Delta x}{2}\right) + (1 - \propto)\left[\frac{1}{2}(Z_j + Z_{j-1})\right]$$

for u<0

$$Z_{j+1/2} = \propto \left(Z_{j+1} + G_x Z_{j+1} \frac{\Delta x}{2}\right) + (1 - \propto)\left[\frac{1}{2}(Z_j + Z_{j+1})\right]$$

$$Z_{j-1/2} = \propto \left(Z_j + G_x Z_j \frac{\Delta x}{2}\right) + (1 - \propto)\left[\frac{1}{2}(Z_j + Z_{j-1})\right]$$

Resulting 1-D Stencil

j-2	j-1	j	j+1	j+2	α	$\dot{m}$
1/4	-5/4	+3/4	+1/4	0	1	>0
0	-1/4	-3/4	+5/4	-1/4	1	>0
+1/6	-6/6	+3/6	+2/6	0	1/2	<0
0	-2/6	-3/6	+6/6	-1/6	1/2	<0

- Slope limiting required when gradients are not smooth (Berger et al, 2005, 43rd AIAA)

7 Linear Residual-Based Stabilization

- Is there a better way that either unstabilized (oscillatory and non-monotonic) and dissipative upwind?
- Consider the model advection/diffusion PDE in the context of a FEM

$$\int w\frac{\partial \rho Z}{\partial t}dV + \int w\frac{\partial \rho u_j Z}{\partial x_j}dV + \int \frac{\partial w}{\partial x_j}\frac{\mu}{Sc}\frac{\partial Z}{\partial x_j}dV - \int w\frac{\mu}{Sc}\frac{\partial Z}{\partial x_j}n_j dS = 0$$

- Concept: Add a scaled fine-scale residual for stabilization, Streamwise Upwind Petrov Galerkin (Hughes and Brooks, 1982)

$$+\sum_{elem}\tau u_k\frac{\partial w}{\partial x_k}\left(\frac{\partial \rho Z}{\partial t}+\frac{\partial \rho u_j Z}{\partial x_j}-\frac{\partial}{\partial x_j}\frac{\mu}{Sc}\frac{\partial Z}{\partial x_j}\right)dV$$

- As noted earlier, CVFEM can be recovered by applying the piecewise-constant test function, w:

$$-\sum_{elem}\tau u_k A_k\left(\frac{\partial \rho Z}{\partial t}+\frac{\partial \rho u_j Z}{\partial x_j}-\frac{\partial}{\partial x_j}\frac{\mu}{Sc}\frac{\partial Z}{\partial x_j}\right)$$

- Godunuv's theorem states that a linear stabilization approach is not sufficient to damp out all osciallations

8 Linear Residual-Based Stabilization

- Is there a better way that either unstabilized (oscillatory and non-monotonic) and dissipative upwind?
- Consider the model advection/diffusion PDE in the context of a FEM

$$\int w\frac{\partial \rho Z}{\partial t}dV + \int w\frac{\partial \rho u_j Z}{\partial x_j}dV + \int \frac{\partial w}{\partial x_j}\frac{\mu}{Sc}\frac{\partial Z}{\partial x_j}dV - \int w\frac{\mu}{Sc}\frac{\partial Z}{\partial x_j}n_j dS = 0$$

- Concept: Add a scaled fine-scale residual for stabilization, Streamwise Upwind Petrov Galerkin (Hughes and Brooks, 1982)

$$+\sum_{elem}\tau u_k\frac{\partial w}{\partial x_k}\left(\frac{\partial \rho Z}{\partial t}+\frac{\partial \rho u_j Z}{\partial x_j}-\frac{\partial}{\partial x_j}\frac{\mu}{Sc}\frac{\partial Z}{\partial x_j}\right)dV$$

- As noted earlier, CVFEM can be recovered by applying the piecewise-constant test function, w:

$$-\sum_{elem}\tau u_k A_k\left(\frac{\partial \rho Z}{\partial t}+\frac{\partial \rho u_j Z}{\partial x_j}-\frac{\partial}{\partial x_j}\frac{\mu}{Sc}\frac{\partial Z}{\partial x_j}\right)$$

- Godunuv's theorem states that a linear stabilization approach is not sufficient to damp out all osciallations

9 Nonlinear Stabilization Approach

- Consider a general transport equation for ϕ
- An artificial viscosity approach is provided with coefficient again related to a fine-scale residual:

$$\sum_e \int_\Omega \nu(\mathbf{R}) \frac{\partial w}{\partial x_i} g^{ij} \frac{\partial \phi}{\partial x_j} d\Omega \qquad g^{ij} = \frac{\partial x_i}{\partial \xi_k} \frac{\partial x_j}{\partial \xi_k} \qquad g_{ij} = \frac{\partial \xi_k}{\partial x_i} \frac{\partial \xi_k}{\partial x_j}$$

FEM-based DCO (Shakib, 91) — Co-variant and contra-variant metric tensors

$$\nu(\mathbf{R}) = \sqrt{\frac{\mathbf{R_k R_k}}{\frac{\partial \phi}{\partial x_i} g^{ij} \frac{\partial \phi}{\partial x_j}}} \qquad \text{or min}\ldots.. \nu^{upw} = C_{upw} (\rho^2 u_i g_{ij} u_j)^{\frac{1}{2}}$$

Coefficient based on local residual — Limit the coefficient based on an upwind analogy

- Piecewise-constant test function for CVFEM (with fourth order-form)

$$-\sum_e \int_\Gamma \nu(\mathbf{R}) g^{ij} \left(\frac{\partial \phi}{\partial x_j} - G_j \phi\right) n_i dS$$

- Similar concept to Guermond's "Entropy-viscosity" approach, 2013
- Can also form an interesting LES model when the viscosity is a function of the k.e. fine scale residual (Guermond and Larios, 2015)

10 Advection Operators: Conclusion

- Without diagonal dominance, lack of monotonicity is noted
- Upwind approaches can help, however, comes at the price of numerical accuracy
- Residual-based approaches, which stem from the FEM literature, are useful candidates for CVFEM

Sandia National Laboratories

Guest Lecture Stanford ME469: Code and Solution Verification

PRESENTED BY

Stefan P. Domino

Computational Thermal and Fluid Mechanics

Sandia National Laboratories

U.S. DEPARTMENT OF ENERGY NNSA

Sandia National Laboratories is a multimission laboratory managed and operated by National Technology & Engineering Solutions of Sandia, LLC, a wholly owned subsidiary of Honeywell International Inc., for the U.S. Department of Energy's National Nuclear Security Administration under contract DE-NA0003525.

2 Code and Solution Verification: Outline

- Elements of a Typical Error-prone Validation Study
- Overview of Code Verification
- Solution Verification
- Structural Uncertainty
- Conclusions

3 Conceptual Challenge: Distinguishing Between Model-form Error, Discretization Error, and Code Error

- One mesh, one model, no code pedigree…

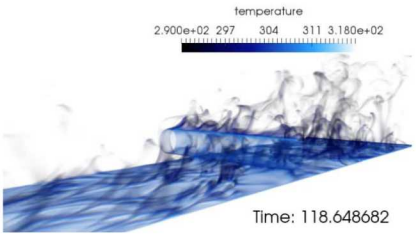

Heat flux to the cylinder
Volume-rendered temperature

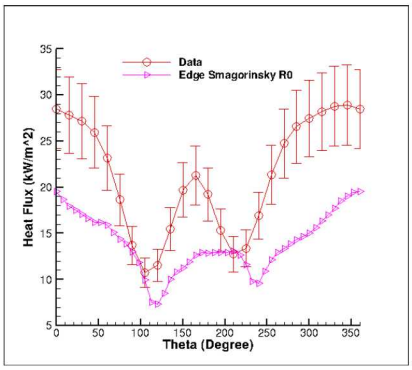

Time-averaged heat flux to cylinder

- What credible scientific hypothesis can be tested in this context?
- Hopefully, a Phenomelogical Identification and Ranking Table (PIRT) was conducted:
  - Process that defines 1) what you know, 2) what you think you know, and 3) what you know not

4 For Transient, Turbulent Flows, Averaging is Required

- The **bane** of turbulent validation: converged statistics require many flow-through times

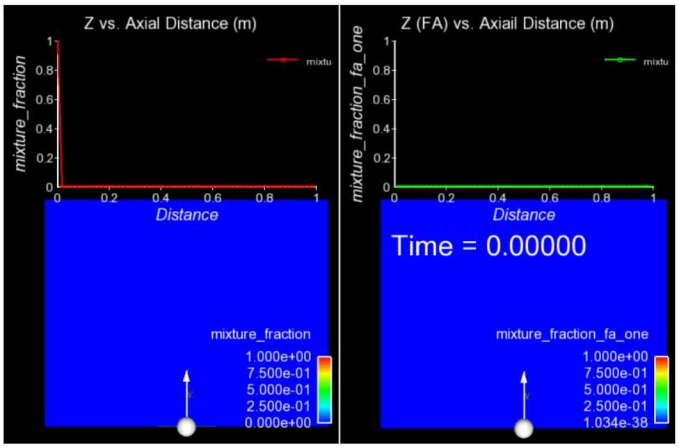

5 Solution Verification and Due Diligence for Model-form (Structural) Uncertainty

- Three meshes, three models
- The heat flux results also show error bars due to time and spatial averaging over a line-of-site

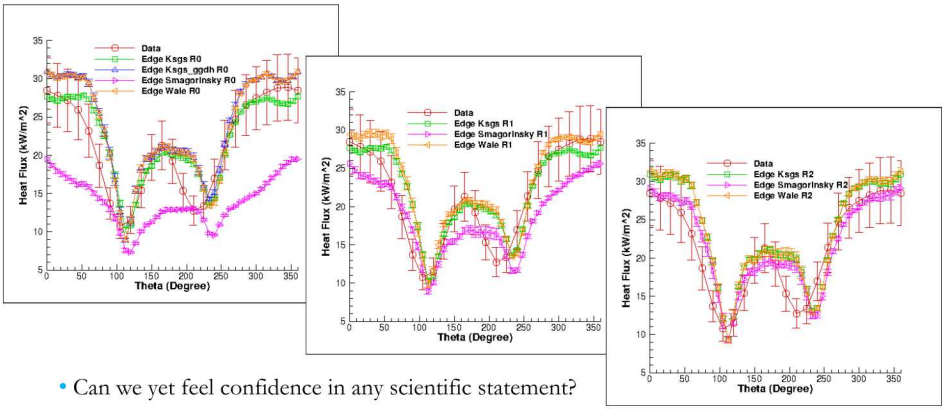

- Can we yet feel confidence in any scientific statement?

6 Essentials of Code Verification

- Taxonomy: One *verifies* code and *validates* models
- Code verification establishes the numerical accuracy of the underlying discretization for the given partial differential equation set
- Code verification seeks to provide the temporal and spatial accuracy of the underlying discretization approach
- For temporal discretization error,
  - a two-state Backward Euler time integrator should be first-order in time, specifically the error should scale with Δt
  - a three-state BDF2 time integrator should scale with Δt^2
  - a multi-stake Runga-Kutta schemes can achieve higher-order accuracy
- For spatial discretization error, a method is design-order if the observed order of accuracy is Δx^{P+1}, where P is the underlying polynomial order for interpolation

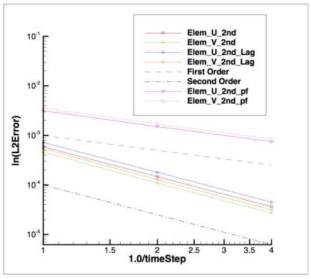

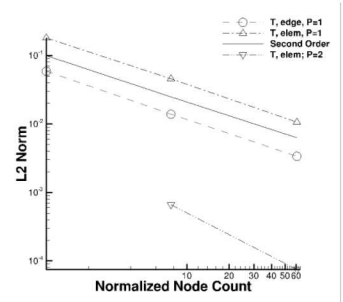

7 Introduction to the Method of Manufactured Solutions (MMS)

How can one provide confidence that the code implementation converges to the proper solution?

- For complex low-Mach fluid flow applications, there are very few analytical solutions
- Consider an approach whereby the solution is manufactured (Roache, et al, 1990)
- Simple thermal heat conduction PDE:

$$\rho C_p \frac{\partial T}{\partial t} - \frac{\partial}{\partial x_j}\lambda\frac{\partial T}{\partial x_j} = 0$$

- with manufactured analytical form for T:

$$T^{MMS} = \frac{1}{4}[\cos(2\alpha\pi x) + cos(2\alpha\pi y) + \cos(2\alpha\pi z)]$$

- Placing this MMS back into model PDE:

$$\rho C_p \frac{\partial T^{MMS}}{\partial t} - \frac{\partial}{\partial x_j}\lambda\frac{\partial T^{MMS}}{\partial x_j} = S^{MMS}$$

provides the source term:

$$S^{MMS} = \frac{\lambda}{4}(2\alpha\pi)^2 cos(2\alpha\pi x)\ cos(2\alpha\pi y) cos(2\alpha\pi z)$$

with error now provided by: $T^E = T - T^{MMS}$

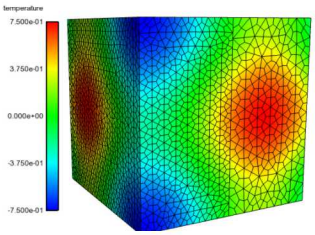

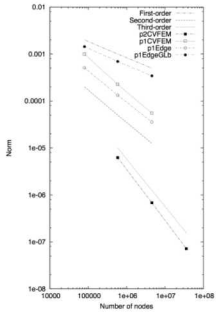

8 Spatial Code Verification for a low-Mach, Variable-Density Flow

- Density is a function of static enthalpy transport via the standard ideal gas, ρ = f(P,M,R,T)
- Temperature range maps to experiment
- Arbitrary buoyancy source term via rotated gravity vector
- Collective study now provides confidence in the interplay between numerical and modeling accuracy

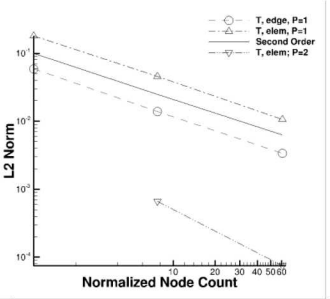

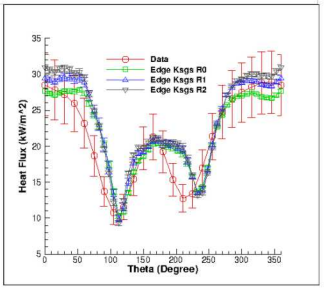

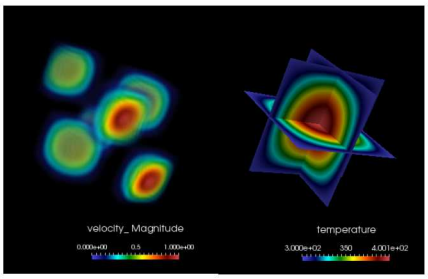

Velocity Mag Temperature

9 The Effect of Polynomial (P) and Mesh Spacing (H) Refinement

- For the heated cylinder-in-cross flow, either mesh resolution or polynomial promotion provides a more accurate result with more turbulence structure

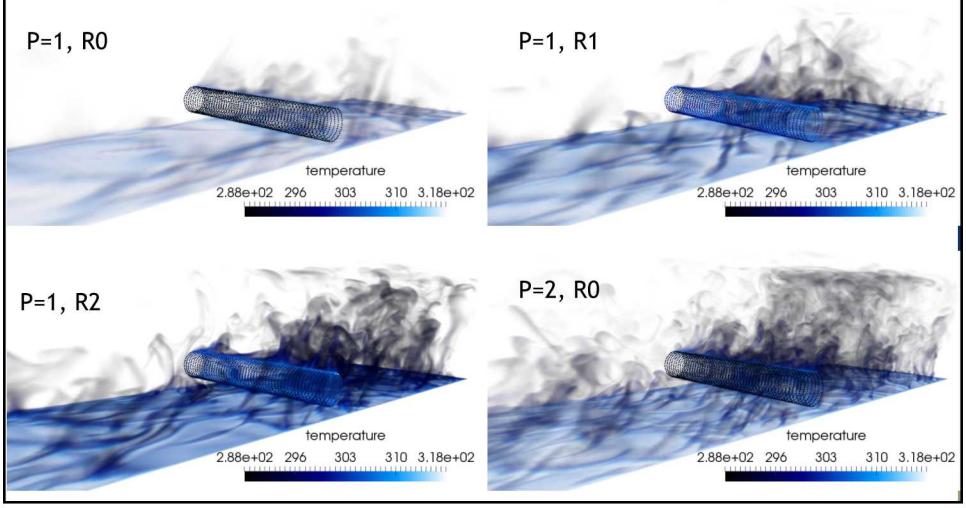

10 Review of a Strong V&V Process

- Objective: Define a sound validation process that includes:
- Definition of key physics, PIRT
- Code implementation
- Code verification
- Solution Verification
- Structural Uncertainty Quantification

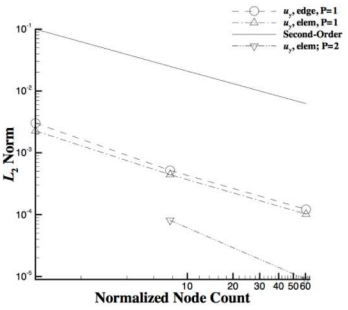

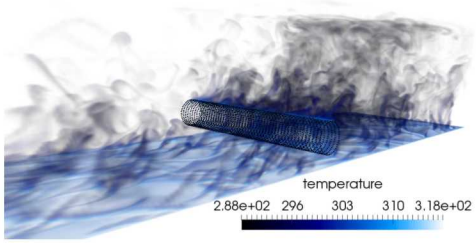

11 More Effective/Efficient Structural Uncertainty

- In the previous high-quality LES validation (cylinder in x-flow), three models were implemented and tested
- Is there a more efficient approach? Yes! Eigenvalue perturbation of the SGS stress

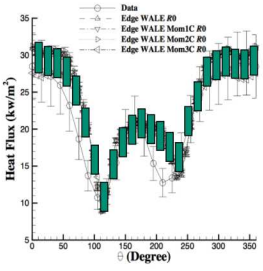

$$\tau_{ij}^{sgs} - \frac{\tau_{kk}^{sgs}}{3}\delta_{ij} = -2\nu_{sgs}\bar{S}_{ij},$$

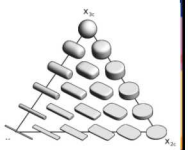

$$a_{ij}^{res} = \frac{1}{\overline{u_k u_k}}\left(\bar{u}_i\bar{u}_j - \frac{\bar{u}_k\bar{u}_k}{3}\delta_{ij}\right) = v_{in}^{res}\Lambda_{nl}^{res}v_{jl}^{res}$$

$$a_{ij}^{sgs} = \frac{1}{\overline{u_k u_k}}\left(\tau_{ij}^{sgs} - \frac{\tau_{kk}^{sgs}}{3}\delta_{ij}\right) = v_{in}^{sgs}\Lambda_{nl}^{sgs}v_{jl}^{sgs},$$

$$\overline{u_i u_j}^{*} = \bar{u}_i\bar{u}_j + \tau_{ij}^{sgs*} = \bar{u}_i\bar{u}_j + \overline{u_k u_k}^{*}a_{ij}^{sgs*} + \frac{\tau_{kk}^{sgs*}}{3}\delta_{ij},$$

with $\overline{u_k u_k}^{*} = \bar{u}_k\bar{u}_k + \tau_{kk}^{sgs*}$ and $a_{ij}^{sgs*} = v_{in}^{sgs*}\Lambda_{nl}^{sgs*}v_{jl}^{sgs*}$.

- See "Framework for characterizing structural uncertainty in LES", Jofre et al, 2017

12 Code and Solution Verification: Conclusions

- Typical validation studies often include one mesh, one model and lack of any code verification
- A validation pedigree includes understanding what models are to be implemented, what code verification is required, and a detailed solution verification
- As a general rule, it takes 10x longer to verify something than to implement the code capability
  - Violations of this rule are abundant– especially when the code implementation is really really hard, e.g., NGP on GPU
- For Structural Uncertainty, i.e., model-form sensitivity, eigenvalue perturbation procedures can be a good approach

Sandia National Laboratories

Guest Lecture Stanford ME469: High Performance Computing for CFD

PRESENTED BY

Stefan P. Domino

Computational Thermal and Fluid Mechanics

Sandia National Laboratories

U.S. DEPARTMENT OF ENERGY NNSA

Sandia National Laboratories is a multimission laboratory managed and operated by National Technology & Engineering Solutions of Sandia, LLC, a wholly owned subsidiary of Honeywell International Inc., for the U.S. Department of Energy's National Nuclear Security Administration under contract DE-NA0003525.

2 High Performance Computing for CFD: Outline

- Overview of Time and Length Scales
  - Fire
  - Wind
- Conceptual Parallel Computing Model
- Types of Scaling: Strong and Weak
- Conclusions

3 Disparity in Time and Length Scales, Fire

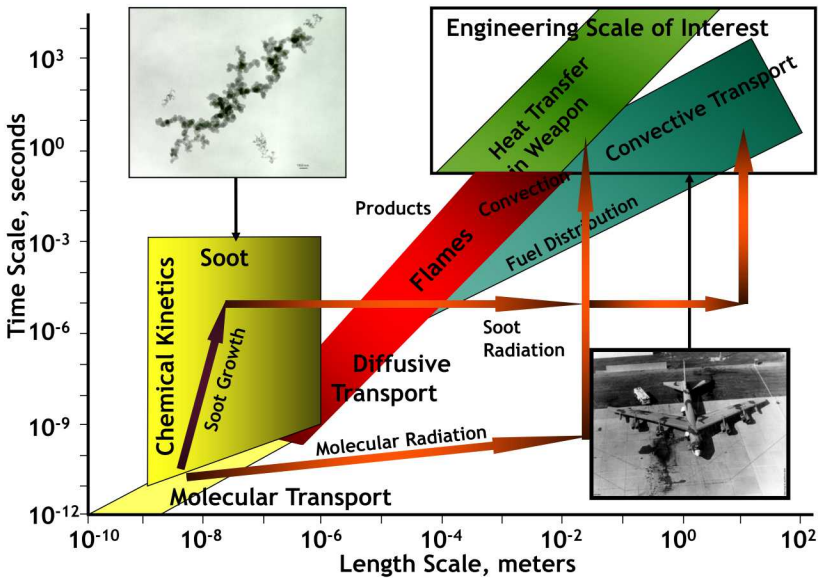

4 Disparity in Time and Length Scales, Wind

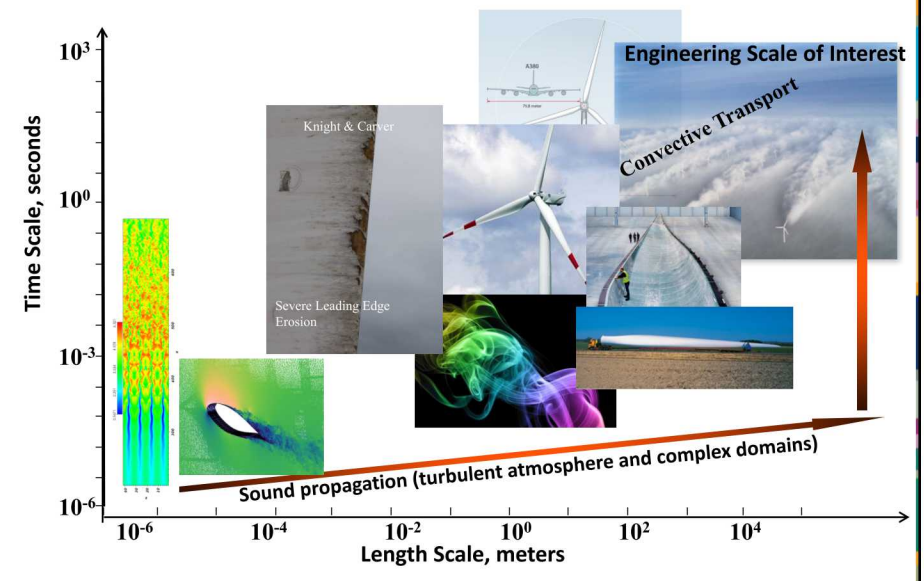

5 High Performance Computing (HPC) Enables Science

- Goal: Paint my house ASAP

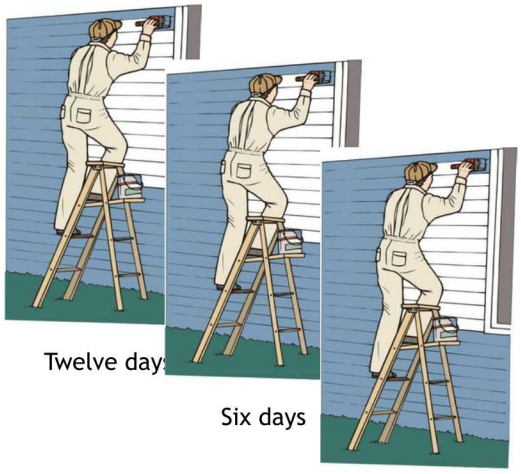

6 Types of Scaling

- Strong Scaling: How the solution time varies with increased computational resources (cores, threads, GPU/Warps) on a fixed-size problem
  - User Y has a mesh that is 1 billion elements and would like to minimize the time it takes to complete a simulation
- Weak Scaling: How the solution time varies with increased problem size on a fixed computational resource load (cores, threads, GPU/Warps)
  - User Y is conducting a validation study that includes three mesh resolutions, which were obtained by uniform mesh refinement, and would like to increase the computational resource appropriately

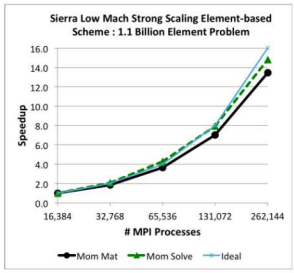

Strong Scaling

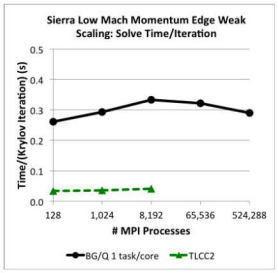

Weak Scaling

7 Challenges Associated with Scaling

- Consider a communication-intensive code procedure: Algebraic Multigrid (AMG) preconditioner setup
- Like verification, the product of a first-time scaling study at a new production scale is generally met with work!

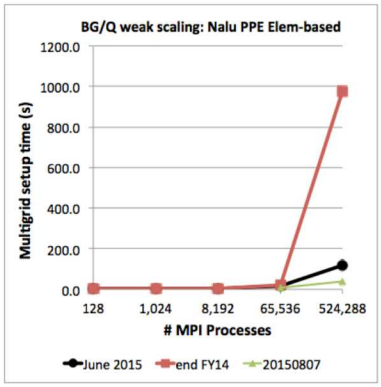

8 High Performance Computing for CFD: Conclusions

- Several fluids applications found in the low-Mach application space require HPC
- Communication bottlenecks can affect scaling
- From a user-perspective, scaling is critical to efficiently deploying production simulation results

Sandia National Laboratories

Guest Lecture Stanford ME469: Multiphysics Coupling

PRESENTED BY

Stefan P. Domino

Computational Thermal and Fluid Mechanics

Sandia National Laboratories

U.S. DEPARTMENT OF ENERGY NNSA

Sandia National Laboratories is a multimission laboratory managed and operated by National Technology & Engineering Solutions of Sandia, LLC, a wholly owned subsidiary of Honeywell International Inc., for the U.S. Department of Energy's National Nuclear Security Administration under contract DE-NA0003525.

2 Multiphysics Coupling: Outline

- Examples of multiphysics coupling with emphasis on fluids, PMR, and CHT
- Monolithic vs Operator Split
- Details of PMR/Fluids Coupling
- Details of PMR/Thermal Coupling
- Details of Fluids/Thermal Coupling
- Verification
- Stability
- Conclusions

3 We Live in a Multiphysics World

- Fluid/Structure coupling:
  - Wind turbines
  - Wing fluttering, etc.
- Non-isothermal fluids/participating media radiation:
  - Fires,
  - Natural gas and coal combustion,
  - Smelting, ethlyne production, etc.
- Conjugate heat transfer:
  - Object-in-fire
  - Gas turbine fine cooling
- Often times, we note a time and length scale disparity
  - For example, consider heating a pan on a home burner
- The coupling architect must generally choose between monolithic and split
- For monolithic, the equations are provided, therefore, the challenge becomes managing a monolithic sytem solve, storage and code design
- For operator split, there can be an "art" in determination of stable couplings due to Eignevalue spread

4 Conjugate Heat Transfer Coupling

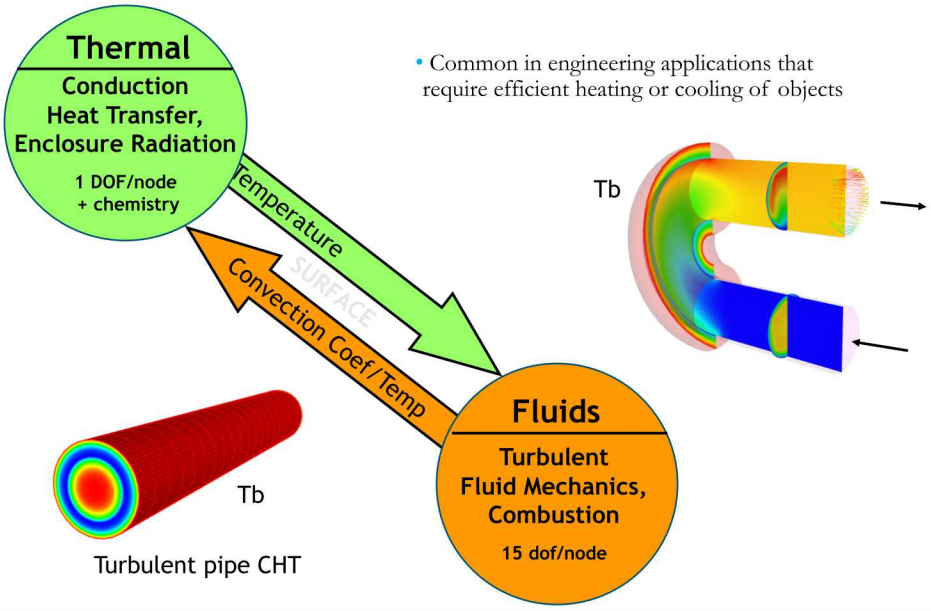

- Common in engineering applications that require efficient heating or cooling of objects

5 Conjugate Heat Transfer Coupling, Equations

- Favre-averaged static enthalpy equation:

$$\frac{\partial \rho h}{\partial t} + \frac{\partial \rho u_j h}{\partial x_j} = -\frac{\partial q_j}{\partial x_j} + \frac{\partial p^t}{\partial t} - \frac{\partial q_j^R}{\partial x_j}$$

- Thermal heat conduction

$$\rho C_p \frac{\partial T}{\partial t} - \frac{\partial}{\partial x_j}\lambda \frac{\partial T}{\partial x_j} = \rho C_p \frac{\partial T}{\partial t} + \frac{\partial}{\partial x_j} q_j^{HC} = 0$$

- Interface condition

$$q_j^{HC} n_j = q_j n_j$$

$$q_n = -\lambda \frac{\partial T}{\partial x_j} n_j = h[T - T^{\infty}]$$

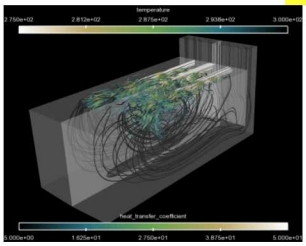

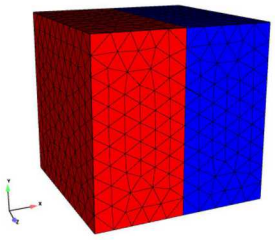

6 Fluid/CHT Coupling Verification

- Unstructured heterogeneous mesh capability
- Arbitrary geometric complexity
- Multi-block domain variable transfer

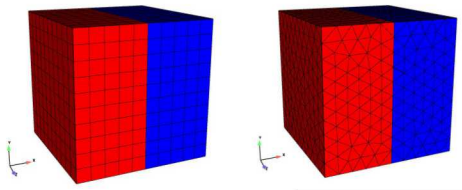

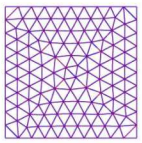

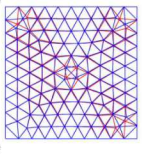

Conforming interface

Non-conforming interface

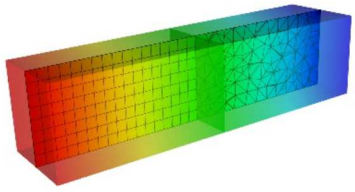

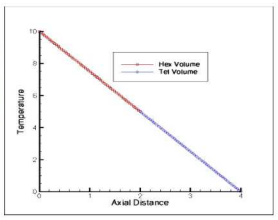

Linear (patch test)

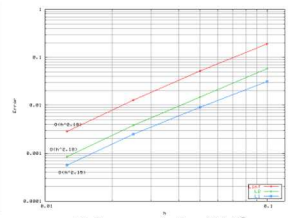

Trigometric MMS

7 Fluids/PMR Coupling

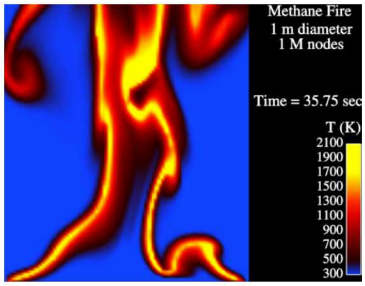

Pool fire

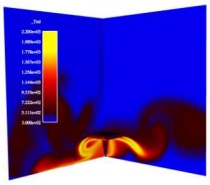

Deflected reacting jet

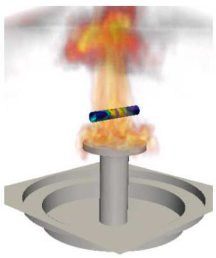

8 Fluids/PMR Coupling Equations

- Favre-averaged static enthalpy equation:

$$\frac{\partial \rho h}{\partial t} + \frac{\partial \rho u_j h}{\partial x_j} = -\frac{\partial q_j}{\partial x_j} + \frac{\partial p^t}{\partial t} - \frac{\partial q_j^R}{\partial x_j}$$

- Steady, non-scattering Radiative Transport Equation

$$s_j^k \frac{\partial I^k}{\partial x_j} + \mu_a I^k = \mu_a \sigma \frac{T^4}{\pi}$$

- Scalar Flux,

$$G \approx \sum_k w_k I^k$$

- Divergence of radiative flux,

$$q_j^R \approx \sum_k w_k I^k s_j^k \qquad \frac{\partial q_j^R}{\partial x_j} = \mu_a [4\sigma T^4 - G]$$

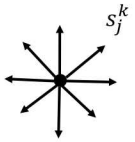

Quadrature

9 PMR/Thermal Coupling

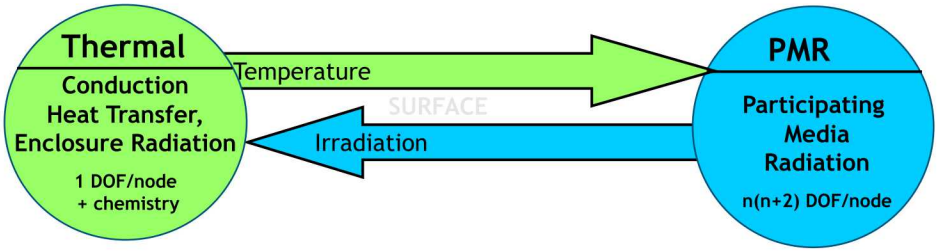

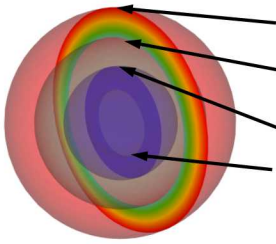

r_o, T_o = 0.1 m, 600K

r_2, T_2 = 0.075 m, 599.291K

r_1, T_1 = 0.05 m, 302.834K

r_i, T_i = 0.03 m, 300K

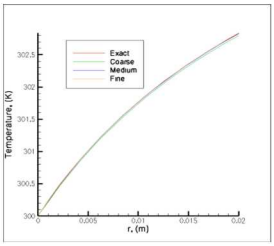

PMR:Conduction through concentric spheres

O(1.8) with faceting,
O(2) without

10 PMR/Thermal Coupling Equations

- Steady, non-scattering Radiative Transport Equation

$$s_j^k \frac{\partial I^k}{\partial x_j} + \mu_a I^k = \mu_a \sigma \frac{T^4}{\pi}$$

- Irradiation (incoming),

$$H \approx \sum_{n_j s_j^k > 0} w_k I^k \left| n_j s_j^k \right|$$

- Grey, diffuse boundary condition (given transmissivity, τ, emissivity ε, and reflectivity, ρ

$$I = \frac{1}{\pi}[\tau \sigma T_e^4 + \varepsilon \sigma T^4 + \rho H]$$

- With boundary condition,

$$q_n = -\lambda \frac{\partial T}{\partial x_j} n_j = \varepsilon [\sigma T_e^4 - H]$$

$$\rho C_p \frac{\partial T}{\partial t} - \frac{\partial}{\partial x_j} \lambda \frac{\partial T}{\partial x_j} = 0$$

11 Conjugate Heat Transfer Stability

- Consider a simple CHT problem

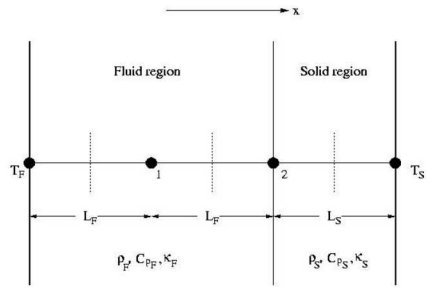

Simplified 1D geometry with 2 nodes for stability analysis of CHT

$$q_n = -\lambda \frac{\partial T}{\partial x_j} n_j = h[T - T^{\infty}]$$

- Compute amplification factor

$$\mathbf{T}^{n+1} = \lambda \mathbf{T}^{n}$$

- Requiring:

$$|\lambda| \leq 1$$

- CHT via flux transfer:
  - Explicit RHS
  - Unstable for certain time steps and material properties
- CHT via convection coefficient:
  - Implicit LHS
  - Unconditionally stable

12 Conjugate Heat Transfer Stability, In Practice

- Transient heated laminar pipe in a 180 degree bend
  - Water, Re = 2000, inflow T = 300
  - Copper jacket, boundary – 350K

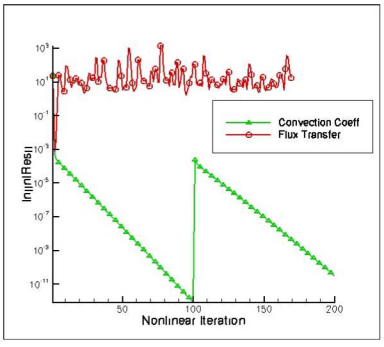

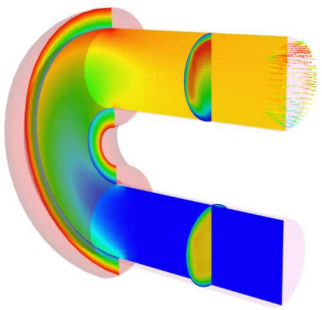

13 Other Linearization Procedures

- PMR and heat conduction radiative boundary condition:

$$q_n = -\lambda \frac{\partial T}{\partial x_j} n_j = \varepsilon[\sigma T_e^4 - H] \qquad lhs \propto \frac{\partial}{\partial T} \varepsilon[\sigma T_e^4 - H] = 4\varepsilon\sigma T_e^3$$

- PMR and fluids coupling, linearized divergence of the radiative flux,

$$\frac{\partial q_j^R}{\partial x_j} = \mu_a[4\sigma T^4 - G] \qquad lhs \propto \frac{\partial}{\partial T} \mu_a[4\sigma T^4 - G] = 16\mu_a\sigma T^3 \frac{1}{C_p}$$

- In practice, such procedures enhance stability for the multi-physics coupling
- In the case of Fluids/CHT, one could possibly monolitically couple the systems
- In the case of Fluids/PMR, monolithic coupling is not practical as the intensity system is ~ N^2, where N is generally O(8)

14 Multiphysics Coupling: Conclusions

- Multiphysics applications are abundant in engineering applications
- Turbulent, reacting flow with PMR and CHT requires a wide range of length and time scale resolution
- Monolithic approaches are ideal from a splitting perspective, however, can be prohibitively expensive when considering systems such as PMR
- Linearization can augment time step stability and should be exploited when possible